SSC18-VIII-06

Guidance, Navigation, and Control for Commercial and Scientific Applications of Formation Flying

Nathan J. Cole, Starla R. Talbot
University of Toronto Institute for Aerospace Studies – Space Flight Laboratory
4925 Dufferin Street, Toronto, Ontario, Canada, M3H 5T6
ncole@utias-sfl.net, stalbot@utias-sfl.net

Faculty Advisor: Dr. Robert E. Zee
University of Toronto Institute for Aerospace Studies – Space Flight Laboratory

ABSTRACT

A guidance, navigation, and control (GNC) system is presented for formation flying missions with variable geometry and fixed time reconfiguration. The drift recovery and station-keeping algorithms developed for the successful CanX-4 and CanX-5 formation flying demonstration are extended to include formation geometries with arbitrary baselines in the along-track and cross-track directions, and to achieve a formation configuration within a specified time. A discussion of the navigation filters used for the CanX-4 and CanX-5 mission is also presented, and the accuracy of a simplified orbit determination technique that would reduce computational complexity and minimize operator involvement is investigated. The added and enhanced capabilities of this ground-based GNC system are described with an emphasis on an operational mission framework designed for scientific and commercial applications. The system is demonstrated with on-orbit data from CanX-4 and CanX-5.

INTRODUCTION

Satellite formations in low earth orbit provide advanced commercial and science opportunities that are difficult or impossible to realize with a single spacecraft. Recently the use of small, multiple coordinated spacecraft has been given much attention as they have the advantage of having lower development times and costs, provide greater mission flexibility, and lead to new and innovative applications. This includes synthetic aperture radar, optical interferometry, on-orbit servicing of other spacecraft, gravitational and magnetic field science, and geolocation.

The CanX-4 and CanX-5 mission, a dual nanosatellite mission developed at the University of Toronto Institute for Aerospace Studies-Space Flight Laboratory (UTIAS-SFL), was the first nanosatellite mission to successfully demonstrate autonomous formation flight with sub-meter control error and centimeter-level relative position knowledge. The spacecraft used cold gas propulsion, an S-band intersatellite communications link, and relative navigation using carrier-phase differential GPS techniques to perform a series of precise, controlled, autonomous formations with separations from 1 km down to 50 m.

CanX-4 and CanX-5 (CanX-4/-5) were launched from Sriharikota India on board the Polar Satellite Launch Vehicle on 30 June 2014. To meet launch vehicle requirements the spacecraft were deployed separately and allowed to drift apart until one spacecraft was ready to begin orbit phasing maneuvers. Prior to the commencing of autonomous formation flying, it was required that the two satellites be brought within a few kilometers of one another. For this purpose, the Drift Recovery And STation Keeping (DRASTK) system was developed to compute fuel-efficient rendezvous trajectories and produce corresponding maneuver commands [1]. DRASTK also provided station-keeping capabilities in the time between individual formation experiments to keep the spacecraft at a safe separation.

This paper presents a guidance, navigation, and control (GNC) system for formation reconfiguration and station-keeping of distributed space systems. A focus on non-autonomous formation flying preserves the ground-based architecture adapted from DRASTK. The updated GNC system extends the success of the CanX-4/-5 technology demonstration to formations with variable geometry and fixed-time configurability. These advances provide capability to maintain arbitrary satellite separation baselines in multiple directions and to establish baselines within a specified amount of time from some initial state. The new operational framework aims to generalize and simplify GNC tasks so that missions of any length can be managed with minimal operator effort. This GNC system is useful for a wide range of commercial and scientific applications, and is

being implemented on upcoming missions such as HawkEye 360 Pathfinder, to which SFL is a contributor. The goal of this mission is radio frequency detection via software defined radios, and signal geolocation using a formation of three satellites.

NAVIGATION

In this section, a method is developed to provide sufficiently accurate orbit estimates using GPS navigation techniques that requires minimal operator input. The proposed method is presented and applied to CanX-4/-5 GPS receiver data during periods where no thrust maneuvers are performed.

The two measurements provided by the GPS receiver used for this orbit determination (OD) are the pseudorange and carrier-phase, obtained by synchronizing the incoming signal with a receiver generated replica. The pseudorange typically has a noise level on the order of 1 m while the carrier-phase has a lower noise level on the order of 1 mm. However, the carrier-phase measurements are ambiguous, due to an unknown integer number of carrier wave cycles between the GPS satellite and receiver that must be estimated along with other parameters. Both the pseudorange and carrier-phase are subject to errors due to atmospheric effects (solely the ionosphere in LEO), instrumental delays in the GPS receiver and GPS satellite, signal multipath errors, and thermal measurement noise.

CanX-4/-5 carried a single frequency GPS receiver. Dual frequency receivers, which may be used on upcoming missions, increase the accuracy of orbit estimates by allowing linear combinations of the pseudorange and carrier-phase which cancel ionospheric error terms, which is a large source of error for the pseudorange. For this analysis an ionosphere-free pseudorange is obtained by taking the arithmetic mean of the pseudocode and carrier-phase measurement (the GRAPHIC combination [2]), which can then be processed similarly to the carrier-phase.

CanX-4/-5 Orbit Determination

CanX-4/-5 employed two on-board navigation filters: a coarse mode extended Kalman filter (EKF), used to determine the absolute position of the CanX-4 and CanX-5 spacecraft individually, and a fine mode EKF, used to provide very accurate estimates of the relative spacecraft state during autonomous formation experiments (on the order of cm and mm/s for relative position and velocity, respectively [3]).

The coarse mode EKF dynamically filtered some of the noise characteristics from the kinematic single point solutions calculated by the GPS receiver, outputting absolute position and velocity states that were smoother than the kinematic solutions. The orbital dynamics model for the coarse mode EKF included first-order gravity, perturbative force acting on the satellite due to higher order gravitational effects (up to a degree and order of 6), and control force due to thrusts [3].

The fine mode EKF filtered raw GPS pseudorange and carrier-phase measurements, and, using a single-difference carrier-phase measurement combination, estimated the relative position and velocity of CanX-5 with respect to the assumed known position of CanX-4, whose state was taken from the GPS receiver. The orbital propagator from the coarse mode EKF was reused for the fine mode.

In addition to the two on-board navigation filters, an offline coarse mode EKF was used to estimate the CanX-4 and CanX-5 spacecraft states. The offline filter served two purposes: the first was to verify that the GPS receiver was functioning as expected during commissioning, and the second was to provide state estimates as input to DRASTK during formation initialization and station-keeping after formation experiments, as the spacecraft were not performing proximity operations during this period. The offline filter, implemented in MATLAB, was similar to the on-board coarse EKF, but used higher order gravity (up to a degree and order 30) and processed forwards and backwards in time as a filter/smoother.

Ground-based Orbit Determination for Operational Formation Missions

For a class of formation flying missions with baseline distances on the order of a kilometer in the along-track direction, on-board autonomous navigation may not be possible or accuracy provided by the relative fine on-board filter may not be necessary. In this case, a ground-based dynamic OD technique can be implemented. This technique builds off the ground-based and on-board CanX-4/-5 coarse mode navigation filter but allows for fully dynamic trajectory modelling. The OD technique should provide a similar level of accuracy as the ground-based coarse EKF and the coarse on-board EKF. It should also minimize operator involvement by automating the process of inputting raw files downlinked from the GPS receiver, retrieving GPS satellite ephemeris files, processing GPS measurements, and outputting orbit estimates to the formation control algorithm. For this, commercially available software is investigated, in this case Analytical Graphics, Inc. Orbit Determination Toolkit (ODTK), to determine if it can provide a similar level of accuracy to the CanX-4/-5 coarse navigation filters. ODTK provides precise force modelling and scripting capabilities to automate the above tasks.

In this OD scheme the relative state is obtained by a direct difference of the CanX-4 and CanX-5 states. Relative states obtained by direct differencing generally experience errors on the order of a few meters [3]. The OD technique used to estimate individual satellite states follows the method in Wright [4] and is implemented in ODTK. An initial orbit determination process generates an initial reference kinematic solution at an epoch using the raw GPS pseudorange from GPS receiver, and precise post-facto ephemeris available from the International GNSS Service (IGS). A dynamic least squares process, which takes the initial orbit estimate and GPS measurements as input, is used to refine the orbit estimate and provide a state error covariance matrix estimate. A forward-time recursive sequential filter method, initialized with the least squares orbit state and covariance matrix, filters the GPS measurements and further refines the orbit estimate and state covariance matrix. The sequential filter uses a Kalman filter measurement update, but the time-update equations use a process-noise based on the uncertainty in the physical models. Finally, the filter output is smoothed to find the best post-fit orbit estimate [4].

Accelerations due to gravitational and non-gravitation forces are modeled. A 100 x 100 EGM2008 static gravity model is used, and accelerations due to atmospheric drag and solar radiation pressure are computed using a spherical model of the satellite. Atmospheric density is computed using the Jacchia 71 density model, and drag coefficient, C_D, and solar radiation pressure coefficient, C_r, are estimated as part of the filtering process to account for deficiencies in the physical models.

The post-fit pseudorange and GRAPHIC combination filter residuals for CanX-4 are shown in Figure 1 (results are similar for CanX-5). No thrust maneuvers were performed during this period. The pseudorange residuals have are zero mean with an RMS of 2.4 m.

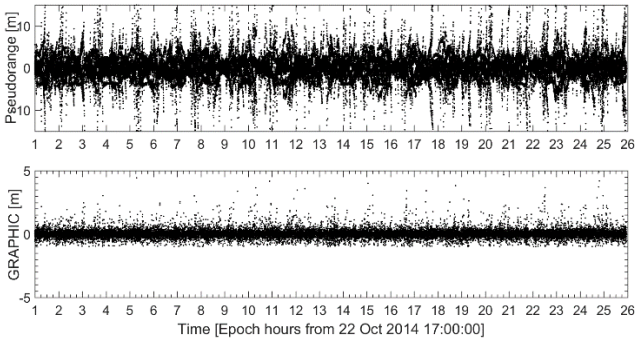

Figure 1: Post-fit Pseudorange Residuals (Top) and GRAPHIC Combination Residuals (Bottom).

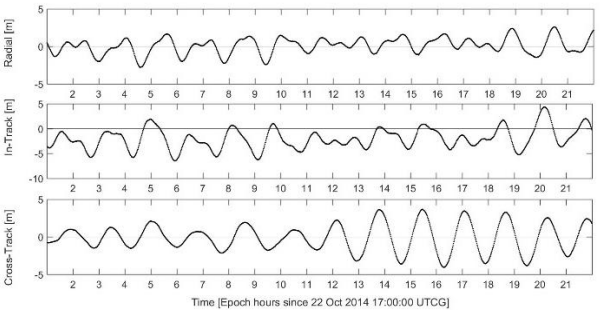

Figure 2: CanX-4: ODTK Position Estimate to Ground Based EKF Position Estimate.

The GRAPHIC measurements are zero mean with an RMS of 25 cm. These pseudorange residuals agree with the CanX-4/-5 residuals computed with the ground-based EKF during formation initialization, which had an RMS error between 0.5 and 2.0 m [1]. The offline navigation filter provided sufficient accuracy to control CanX-5 with a relative error of less than 2 km to CanX-4 when the two satellites were within 30 km of each other [1]. Figure 2 shows the position of CanX-4 obtained from ODTK to the position estimated with the offline coarse EKF in the Radial, In-Track, and Cross-Track (RIC) reference frame. The two orbit estimates agree to within 5 m. The in-track component has a bias of about 2 m, which could be due to mis-modeling in the atmospheric drag model and process noise that is too optimistic in ODTK. The velocity estimates, not shown, agree with the ground based EKF to within 10 cm/s in each component.

Table 1 shows a comparison of the relative state of CanX-4 and CanX-5 found from differencing the absolute states estimated with ODTK and the relative state estimated from the on-board fine mode EKF. The accuracy of the ODTK orbit estimates is about 2 m when compared to the fine mode EKF.

Although these results are generally in agreement with relative orbit determination through the direct differencing of absolute orbit states [3], they represent an upper bound of acceptable accuracy based on the CanX-4 and CanX-5 mission. There are several ways to increase the orbit determination accuracy if required. Within the filter process, outlying observations are excluded from the next measurement step if their residual exceeds a 3-sigma level relative to the unweighted RMS of all accepted observations computed in the previous steps, which provides some filtering of

Table 1: Comparison of Relative Orbit Estimates

Differential Component	Mean [m]	RMS [m]
Radial	0.01	1.1
In-track	1.9	2.3
Cross-track	-0.03	0.3

noisy measurements. GPS data editing to screen outliers and bad measurements could also be implemented. Within the current OD scheme, a user configurable threshold can be used to discard any observation below a minimum signal-to-noise ratio. Observations below a certain elevation mask (e.g. 5°) could also be discarded. There are precise OD methods which use reduced dynamic techniques where an a-priori orbit is determined from dynamically smoothing single point navigation solutions with high fidelity force models. Additionally, during filtering, empirical accelerations, which are stochastic parameters employed to compensate for any deficiencies in the dynamical model, are also adjusted [5]. The a-priori orbit estimate is then used to identify any outlying pseudorange measurements and detect cycle slips in the carrier-phase measurements. These techniques generally achieve accuracies on the order of centimeters (for both single and dual frequency receivers) [5] but require greater computational complexity.

A measure of adequacy of this OD technique is the error in the relative semi-major axis, since differences in the semi-major axis lead to undesirable differential along-track drift. A derivation of the error in the differential semi-major axis $\sigma_{\Delta a}$ is presented in [6] and given by

$$\sigma_{\Delta a} = 2\sqrt{4\sigma_x^2 + \frac{4}{n}\rho_{x\dot{y}}\,\sigma_x\sigma_{\dot{y}} + \frac{1}{n^2}\sigma_{\dot{y}}^2} \qquad (1)$$

where σ_x is the radial position, $\sigma_{\dot{y}}$ is the along-track velocity, and $\rho_{x\dot{y}}$ is the correlation between the radial position and along-track velocity. Station-keeping accuracy on the order of a kilometer requires a value of $\sigma_{\Delta a}$ of about 0.3 to 1.0 m. With the presented OD method, the differential semi-major axis error is about 0.5 m, which translates into a drift of 5 m/orbit. Here, the values of σ_x, $\sigma_{\dot{y}}$, and $\rho_{x\dot{y}}$ are computed by comparing the relative state obtained with ODTK to precise orbit states computed independently on the ground.

GUIDANCE AND CONTROL

Satellite formation flying is the coupled control of one satellite's dynamic state with respect to another [7]. This requires a state parameterization and motion model that represents the relative dynamics of the satellite formation with acceptable fidelity to meet mission requirements. Using this relative state parameterization and motion dynamics model, the satellite formation geometry is configured and maintained according to a guidance and control algorithm that considers the operational constraints of a specific mission. In 2014, CanX-4/-5 mission demonstrated precision formation flying capabilities using the DRASTK algorithm. This section of the paper discusses the evolution of DRASTK to extend its capabilities towards commercial and scientific applications of distributed space systems in LEO.

Extending DRASTK Capabilities

The DRASTK algorithm was responsible for performing the formation initialization and station-keeping tasks for CanX-4/-5. DRASTK is implemented in MATLAB and interfaces with Analytical Graphics, Inc. Systems Tool Kit (STK) software to aid in the trajectory optimization and maneuver planning required to achieve a desired formation. DRASTK's reconfiguration plan is constructed in three phases [1]:

1) establish a differential mean semi-major axis to initiate drift towards a desired relative along-track position;
2) establish a differential mean inclination to initiate drift towards a desired relative mean right ascension of the ascending node (RAAN); and,
3) compute eccentricity and argument of perigee correction maneuvers at optimal times during the drift phase.

DRASTK then performs minor trajectory corrections and arrests drift in relative RAAN and relative along-track separation at the required time. The completed guidance plan is then taken with current orbital states of the satellites, thrust magnitude constraints, and thrust timing constraints to compute the required maneuvers that are uploaded to the spacecraft.

Extending the capabilities of DRASTK requires a few key developments. The algorithm must be generalized to control a range of formation geometries within the LEO environment, whereas CanX-4/-5 only demonstrated formation rendezvous and proximity operations [1]. This requires extending the formation control to maintain configurations with arbitrary inter-satellite separations. In addition to constraining thrust times to be within specified intervals, the capability to achieve configurations within a specified time is required. Similarly, with payload operations being paramount, station-keeping control must be an unobtrusive process within mission operations. Lastly, since industrial missions can have lifetimes of years opposed to months, the algorithm must be as automated as possible so that

implementation is achieved with minimal operator effort and more deterministic run-times.

Building off DRASTK, this updated guidance and control algorithm is a ground-based system that uses MATLAB as the scripted language to perform numerical computations and interface with STK's high fidelity simulation environment. This method extends LEO formation control to include geometries with arbitrary baselines in the along-track and cross-track directions. It also adopts a generalized approach to including perturbations within the dynamic relative motion through a state transition matrix (STM) and updated relative orbital element (ROE) state parameterization. Lastly, the method allows for straight-forward inclusion of time constraints that are accounted for directly in the maneuver planning to automate operation as much as possible.

State Parameterization and Relative Astrodynamics

The choice of relative state parameterization for satellite formation flying was informed by a comprehensive survey and assessment of relative motion dynamics models by Sullivan et al., and consideration of operational requirements for upcoming SFL formation flying missions, such as the HawkEye 360 Pathfinder mission. The literature shows that orbital element based models offer simpler inclusion of secular perturbation effects and their linearized relative dynamics capture formation motion more accurately than translational models [8].

Considering this, a relative orbital element (ROE) state parameterization is used [9], given as

$$\delta\boldsymbol{\alpha} = \begin{bmatrix} \delta a \\ \delta\lambda \\ \delta e_x \\ \delta e_y \\ \delta i_x \\ \delta i_y \end{bmatrix} = \begin{bmatrix} (a - a_{ref})/a_{ref} \\ \left(u - u_{ref}\right) + \left(\Omega - \Omega_{ref}\right)\cos i_{ref} \\ e\cos\omega - e_{ref}\cos\omega_{ref} \\ e\sin\omega - e_{ref}\sin\omega_{ref} \\ i - i_{ref} \\ \left(\Omega - \Omega_{ref}\right)\sin i_{ref} \end{bmatrix} \quad (2)$$

where a, e, i, M, ω, and Ω denote the mean Keplerian elements and $u = \omega + M$ is the mean argument of latitude. Note that all orbital element parameters in the remainder of this work are assumed to be mean elements. In Eq. (2): δa, $\delta\lambda = du + di_y \cot i$, δe_x and δe_y, and δi_x and δi_y represent the non-dimensional relative semi-major axis, relative mean longitude, components of the relative eccentricity vector ($\delta\boldsymbol{e}$), and components of the relative inclination vector ($\delta\boldsymbol{i}$) respectively. The *ref* subscript denotes the reference satellite of the ROE state. Within the context of this guidance and control algorithm, the reference satellite represents a controlled satellite that undergoes impulsive maneuvers and the other satellite is uncontrolled, subject only to natural dynamics of the orbit environment.

Relative motion can be expressed in a rotating rectilinear Radial, Tangential, Normal (RTN) frame centered on the reference satellite to offer direct insight on formation geometry. From the ROE state: δa and $\delta\lambda$ describe satellite separation in the radial (R) and along-track (T) directions, respectively, while the magnitudes of $\delta\boldsymbol{e}$ and $\delta\boldsymbol{i}$ vectors describe the in-plane (RT) and out-of-plane/cross-track (N) oscillation amplitudes, respectively [10]. An additional insight on formation motion is afforded by the angular separation of relative eccentricity and inclination vectors. An elliptical relative motion results from the phase difference of in-plane and out-of-plane harmonic oscillations as a function of the reference satellite's mean argument of latitude u – this motion can be configured to ensure passive safety between satellites by making $\delta\boldsymbol{e}$ and $\delta\boldsymbol{i}$ (anti-)parallel [11]. This differs from how DRASTK set up passive safety using the Hill-Clohessy-Wiltshire (HCW) equations [1]. These geometric insights allow the ROE state to offer both the intuitive Cartesian representation of formation geometry and motion for mission-level design, and the greater fidelity and simplicity of differential orbital elements for formation control.

The linearized relative dynamics for the ROE state are described by a corresponding STM [9]. This STM captures the effects of secular drift in absolute orbital elements due to Keplerian dynamics (mean orbital motion) and the J_2 perturbation (mean anomaly, argument of perigee, and RAAN), described in Eq. (3) and Eq. (4) respectively,

$$\dot{M}_{kep} = n = \sqrt{\mu/a^3} \quad (3)$$

$$\begin{bmatrix} \dot{M} \\ \dot{\omega} \\ \dot{\Omega} \end{bmatrix}_{J_2} = \frac{3}{4}\frac{J_2 R_E^2 \sqrt{\mu}}{a^{7/2}(1-e^2)^2} \begin{bmatrix} \sqrt{1-e^2}(3\cos^2 i - 1) \\ 5\cos^2 i - 1 \\ -2\cos i \end{bmatrix} \quad (4)$$

where μ is Earth's standard gravitational parameter, $J_2 = 1.0826 \times 10^{-3}$, and R_E is the Earth's radius. Relative dynamics are linearized through first-order Taylor series expansion of the time derivatives of $\delta\boldsymbol{\alpha}$ due to Keplerian and J_2 effects, about zero satellite separation ($\delta\boldsymbol{\alpha} = 0$). The resulting STM is valid for arbitrary separations in $\delta\lambda$ and δi_y but requires small separations in δa, δe_x, δe_y, and δi_x [9]. This range of validity is ideal for formation flying applications where satellites are in arbitrarily eccentric orbits of nearly identical shape but have any range of mean anomaly and RAAN – the satellites can be distributed to any position along their orbit and to any node along the equator. Note that this ROE state is singular when the uncontrolled satellite is

in an equatorial orbit [9], but this is not a concern for missions that makes use of inclined orbits (e.g. Sun synchronous orbits).

A method of STM derivation used by Koenig et. al can be applied to incorporate any perturbations into the ROE motion model through the Gauss variational equations (GVE), such as differential atmospheric drag or solar radiation pressure. For example, augmenting the ROE state with time derivatives of the ROE parameters effected by differential atmospheric drag allows these secular effects to be included in an expanded density-model-free STM for orbits of arbitrary eccentricity [9].

$$\delta\boldsymbol{\alpha}_{aug} = \left[\delta\boldsymbol{\alpha}_{qns}^{T} \;\; \delta\dot{a}_{drag} \;\; \delta\dot{e}_{x_{drag}} \;\; \delta\dot{e}_{y_{drag}}\right]^{T} \tag{5}$$

where $\delta\dot{a}_{drag}$, $\delta\dot{e}_{x_{drag}}$, $\delta\dot{e}_{y_{drag}}$ are the respective differential drag drift rates of the relative semi-major axis and relative eccentricity vector, augmenting the ROE state. This differential drag augmented motion model is used for missions involving satellites with varied ballistic coefficients at low enough altitudes. Drag augmented state parameters are evaluated at the same time as the numerical mean orbital elements are calculated from the dynamic position and velocity state provided by the navigation system.

Impulsive maneuvers perturbing the reference satellite's absolute state are also incorporated into the ROE motion model using the GVE. The effects of small velocity changes (Δv) in the RTN frame due to thrust maneuvers are approximated for near-circular orbits as control disturbances in the ROE state ($\Delta\delta\boldsymbol{\alpha}$) through a control matrix [10]

$$\Delta\delta\boldsymbol{\alpha}_k = \frac{1}{na}\begin{bmatrix} 0 & 2 & 0 \\ -2 & 0 & 0 \\ \sin u_k & 2\cos u_k & 0 \\ -\cos u_k & 2\sin u_k & 0 \\ 0 & 0 & \cos u_k \\ 0 & 0 & \sin u_k \end{bmatrix}\begin{bmatrix}\Delta v_R \\ \Delta v_T \\ \Delta v_N\end{bmatrix} \tag{6}$$

where n is the mean orbital motion, a is the reference satellite's semi-major axis, u_k is the mean argument of latitude at thrust time t_k, and Δv_{RTN} are the small velocity variations in the radial, along-track, and cross-track directions, respectively, introduced by control thrusts along respective RTN axes. Note that mean argument of latitude is more useful than time as the independent variable in this control matrix for maneuver planning (although the secular J_2 effects must be accounted for when substituting Δu for Δt in the STM). This control matrix makes use of the linearized ROE assumption to superimpose maneuver dynamics with natural relative dynamics through propagation with the STM [10]. It is evident from Eq. (6) that, assuming a near-circular orbit, the linearized ROE motion model decouples in-plane (RT) and out-of-plane (N) formation control.

Formation Guidance

Formation guidance seeks to plan a trajectory from an initial ROE state, $\delta\boldsymbol{\alpha}_0$, to a final desired ROE state, $\delta\boldsymbol{\alpha}_f$, by passing through a set of m intermediate ROE states, $\delta\boldsymbol{\alpha}_k$, at specific times t_k (for $k = 1, \dots, m$), while minimizing the total fuel expenditure [12]. The minimum fuel optimization is considered in terms of a minimization of change in ROE due to control maneuvers, $\Delta\delta\boldsymbol{\alpha}_k$ – these are proportional, as understood from Eq. (6), since $\Delta\delta\boldsymbol{\alpha}$ is directly related to the Δv resulting from fuel expenditure. The optimization problem is written as

$$\min_{\Delta\delta\boldsymbol{\alpha}_k} J_{guid} = \sum_{k=1}^{m}(\|\Delta\delta a\|_k)^2 + \sum_{k=1}^{m}(\|\Delta\delta\lambda\|_k)^2 + \sum_{k=1}^{m}(\|\Delta\delta\boldsymbol{e}\|_k)^2 + \sum_{k=1}^{m}(\|\Delta\delta\boldsymbol{i}\|_k)^2 \tag{7}$$

and subject to equality constraint

$$\delta\boldsymbol{\alpha}_f = \Phi(t_f, t_0)\delta\boldsymbol{\alpha}_0 + \textstyle\sum_{k=1}^{m}\Phi(t_f, t_k)\Delta\delta\boldsymbol{\alpha}_k \tag{8}$$

where $\Phi(t_2, t_1)$ is the STM discussed in the previous section over time interval $\tau = t_2 - t_1$. This ground-based guidance algorithm employs numerical optimization to solve for the minimal ROE variations, $\Delta\delta\boldsymbol{\alpha}_k$, opposed to a closed-form analytical solution using a simplified STM that neglects cross coupled relative dynamics between in-plane and out-of-plane ROE parameters [10]. Leveraging the functionality provided by implementing the GNC algorithm in MATLAB, a constrained linear minimization function is used to fully exploit the relative dynamics to obtain a fuel-optimal guidance plan. Once the fuel-optimal ROE increments, $\Delta\delta\boldsymbol{\alpha}_1, \dots, \Delta\delta\boldsymbol{\alpha}_m$, have been solved for, the intermediate ROE states of the guidance trajectory can be reconstructed using:

$$\delta\boldsymbol{\alpha}_k = \Phi(t_k, t_{k-1})\delta\boldsymbol{\alpha}_{k-1} + \Delta\delta\boldsymbol{\alpha}_k,\ k = 1, \dots, m \tag{9}$$

Formation Control

Formation control seeks to compute the fuel-optimal set of N impulsive maneuvers, Δv_j for $j = 1, \dots, N$, that bring the ROE state from some initial $\delta\boldsymbol{\alpha}_{k-1}$ to the next configuration in the guidance plan, $\delta\boldsymbol{\alpha}_k$, over the control period from t_{k-1} to t_k, while respecting constraints for

time intervals in which no thrusts can occur. The cost of this incremental reconfiguration is given by

$$\Delta\delta\boldsymbol{\alpha}_k = \sum_{j=1}^{N} \Phi(t_k, t_j)\Delta\delta\boldsymbol{\alpha}_j \quad (10)$$

This control algorithm employs either one of two methodologies to compute maneuver time and location, direction, and magnitude: a semi-analytical method resulting in a fuel-optimal set of four maneuvers, and a more computationally intensive numerical method resulting in a variably numbered set of fuel-optimal maneuvers.

The semi-analytical control method is based on the closed-form solutions developed by Chernick and D'Amico, which compute a fuel-optimal solution of three in-plane thrusts and a single out-of-plane thrust [10]. This semi-analytical algorithm constrains in-plane maneuvers to tangential thrusts (Δv_T), and the out-of-plane maneuver is a normal thrust (Δv_N), which makes use of the decoupled control arising from the near-circular orbit assumption of Eq. (6). The semi-analytical control method determines the optimum time (in terms of mean argument of latitude location, u_N) for the out-of-plane maneuver based on the phase of the desired change in the inclination vector, $\Delta\delta\boldsymbol{i}$,

$$u_N = \arctan(\Delta\delta i_y / \Delta\delta i_x) \quad (11)$$

and, through an iterative process, refines this location considering J_2 effects and the current argument of latitude of the satellite [10]. The optimum times for the set of in-plane maneuvers are determined by the phase of the desired change in the eccentricity vector, $\Delta\delta\boldsymbol{e}$,

$$u_{T_j} = \arctan(\Delta\delta e_y / \Delta\delta e_x) + m_j\pi \quad (12)$$

and occur at integer multiples, m_j, of half the orbital period [10]. All possible triplets of u_{T_j} (for $j = 1, 2, 3$) are computed within the allowable control period and the corresponding least-squares solutions of total Δv_{T_j} is computed by inverting Eq. (10) to solve for $\Delta\boldsymbol{v}$ in Eq. (6). The minimum calculated $\sum_{j=1}^{N} \Delta\boldsymbol{v}_j$ out of all the computed sets of four maneuvers represents the fuel-optimal control solution, within the assumptions of this semi-analytical control method.

The numerical control method adopts the primer vector theory algorithm designed by Roscoe et. al to converge on the minimum-fuel set of *N* maneuvers [13]. There are no restrictions placed on thrust direction or timing, other than enforcing the time/location intervals where no thrusts are allowed and a minimum time between thrusts. The optimal reconfiguration is refined by relating a discrete-time solution to a continuous-time solution and iterating from the primer vector history until the number of discrete thrusts and their corresponding times and locations, magnitudes, and directions converge to fuel-optimality. The convergence conditions can be set based on mission priorities, since sub-optimal solutions still accomplish the desired control variations in the ROE state for a given control period [13]. Considerations used to inform convergence criteria might include: maximum number of iterations, minimum total fuel cost, number of maneuvers, thrust magnitude limits, or minimum time between thrusts.

Reconfiguration Operations

The goal for the guidance and control algorithm during reconfiguration phases of a mission is to bring the formation from some arbitrary initial state to some desired state within a fixed period of time in a fuel optimal way. These operational phases occur for various reasons related to mission or payload operations, including: initializing the formation after deployment from the launch vehicle and uncontrolled drift during commissioning, changing baseline lengths for payload observations, orbit raising, along-track position changes within the formation to accommodate the addition/loss of satellites, and swapping the position of satellites with different payload functions.

As previously discussed in the *Formation Guidance* section, a reconfiguration trajectory is planned with intermediate configuration waypoints specified periodically. The time discretization of this reconfiguration trajectory has operational implications that must be considered. Longer control windows between intermediate configuration waypoints can result in an inconsistency between along-tack offset ($\delta\lambda$) near the end of a waypoint period and the relative mean semi-major axis (δa) goal at the upcoming waypoint. To avoid requiring large correction maneuvers at the end of a waypoint period, a finer time discretization maintains a smooth change in δa that is consistent with the $\delta\lambda$ values at waypoints. This is more in-line with the assumption of small impulsive control maneuvers – operationally this results in more uniform thrusts over the control period, as depicted in Figure 3.

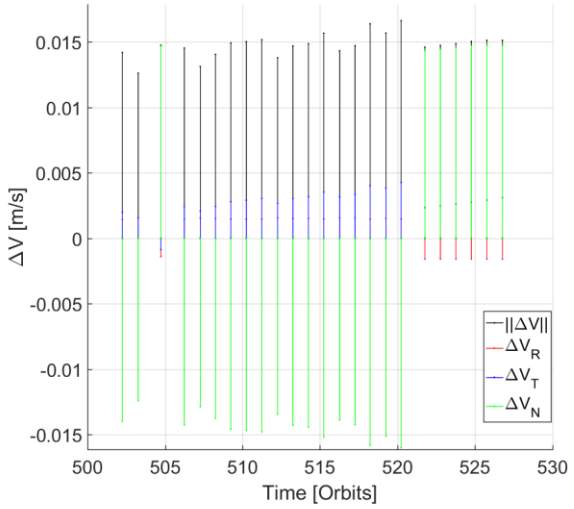

Figure 3: Thrust Plan for an Intermediate Configuration Control Period

For fixed-time reconfiguration, the intermediate waypoints may be far enough apart that the propulsion system cannot physically realize the required four-thrust maneuver solution required. This can occur during reconfigurations with aggressive time constraints, such as a short initialization phase. When this is the case, the numerical control method, discussed in the *Formation Control* section, can provide a control solution with more thrusts of lower magnitude that can be achieved by the propulsion system and offer the fuel-optimal solution, which respects time-constraints. An example of this is provided in Figure 4, where the numerical method converges on a solution of 33 thrusts that still provides near fuel-optimality when compared to an analytical minimum [10].

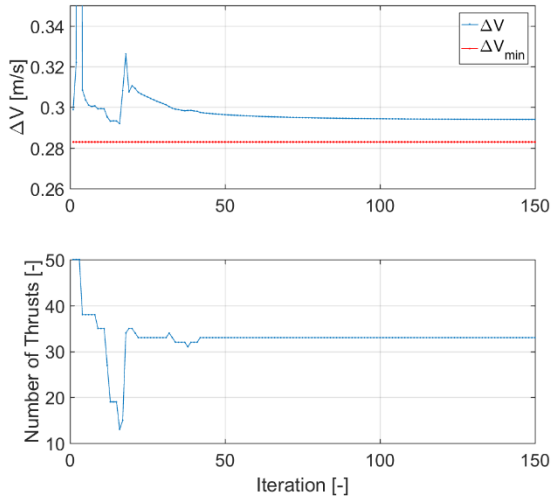

Figure 4: Numerical Control Method Solution

Note that the Δv_{min} lower bound in Figure 4 is for the in-plane maneuver set and is based on tangential thrusts only. Due to this, it is not guaranteed to be the absolute minimum solution and sometimes the numerical control method can improve upon it, as it considers thrusts in any direction. Nevertheless, this analytical Δv_{min} is a good way to assess fuel optimality of the computed solution.

Another operational consideration when using the numerical control method is thrust spacing, and consequently the number of total thrusts allowed during a control window. The propulsion system may specify requirements for the maximum frequency of thrusting due to thermal considerations or actuation cycles, and these operational constraints must also be accounted for in the control solution. A minimum thrust spacing can be specified to limit the number of maneuvers, resulting in fewer overall thrusts that are larger in magnitude and more spaced-out.

Making use of the ground-based formation guidance, STK's high fidelity orbit propagation environment is used to forecast relative trajectories during reconfiguration. This allows for comparison of on-orbit performance with simulated results, but also provides the ability to verify formation safety over the entire reconfiguration. This is important since passive safety in the plane perpendicular to along-track motion is only enforced at the end state of reconfiguration. If there is a potential proximity risk between satellites during reconfiguration, this will be observable in the forecasted relative trajectories and the risk can be mitigated.

Station-Keeping Operations

During station-keeping phases of a mission the guidance and control algorithm must efficiently maintain the desired formation configuration, within specified tolerances, to enable payload operations. During a station-keeping open-loop control period, maneuvers are limited to a few consecutive orbits so that remaining time can be dedicated to payload operations and communication windows, during which no thrusts may occur. This requires the control method to provide a maneuver solution that sets up an ROE state that bounds drift within an acceptable tolerance of formation baseline geometry. These control bounds are defined by mission requirements and directly impose constraints on the length of the station-keeping period based on the minimum impulse bit of the propulsion system and relative drift environment. Alternatively, the tolerable control bounds can be informed by a required station-keeping period if this is a more pertinent constraint due to payload operation times.

When targeting fuel efficient station-keeping maneuvers that exploit the accepted control bounds, relative in-

plane motion over the station-keeping period must be considered. The along-track drift rate, $\delta\dot{\lambda}$, is dictated mainly by the relative mean semi-major axis, δa – along-track control bounds are targeted through maneuvers that adjust δa to achieve the desired drift. The control bounds for $\delta \boldsymbol{e}$ dictate the relative radial oscillation magnitude used to ensure passive safety in the plane perpendicular to along-track motion. The phase angle between the components of $\delta \boldsymbol{e}$ drift at the secular rate of change of the reference satellite's argument of perigee. Therefore, maintaining passive safety requires targeting maneuvers that keep this phase angle as (anti-)parallel to the $\delta \boldsymbol{i}$ phase angle as possible over the station-keeping period. The out-of-plane inclination vector requires no adjustment and can be retargeted continuously at the desired cross-track baseline length. There should be very little drift in δi_y since it is dependent on δi_x – recall that the STM requires small values of δi_x (nominally $\delta i_x = 0$) for the relative dynamics to be valid with the ROE state. Figure 5 is a graphical representation describing the time-evolution of the ROE state due to first-order J_2 perturbation.

If differential drag effects cause further in-plane drift, these effects can be included in the targeting of maneuvers based on navigation data. In this case, along-track drift becomes quadratic as a function of linear secular change in δa – this $\delta\dot{a}$ can be considered constant over a period of ten orbits before propagation error in along-track separation exceeds a few hundred meters [9]. There is also a linear drift in $\delta \boldsymbol{e}$ parallel to the reference satellite's argument of perigee angle, related to the circularizing of orbits due to atmospheric drag [9].

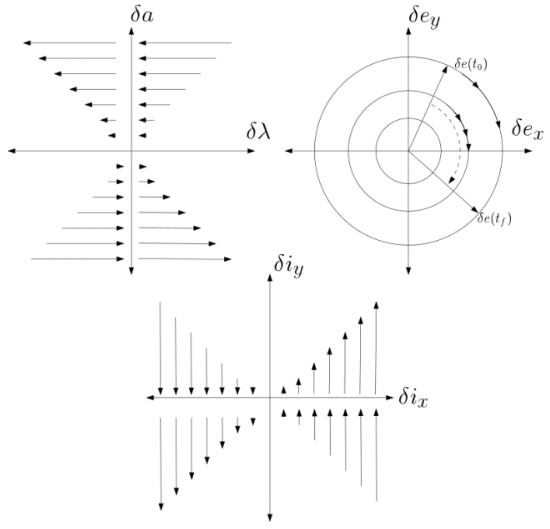

Figure 5: ROE Drift Due to First-Order J_2 Perturbation

Again, making use of the computational capabilities of a ground-based formation guidance method, STK's simulated relative trajectories offer forecasting of extended open-loop station-keeping periods and the ability to compare performance from on-orbit ephemeris to high fidelity simulation predictions.

Reconfiguration Simulation Results

As part of the algorithm framework, STK is used as a high fidelity orbit propagation environment. Control solutions computed for reconfiguration scenarios are implemented in STK to verify that end states are achieved successfully in a simulated truth model. This truth model is used to provide representative ephemeris to the algorithm for future control periods so that satellite trajectories can be forecasted to compare with eventual on-orbit ephemeris. This forecast is also the basis for a formation situational awareness procedure used to inform operators of any upcoming issues before they occur. This forecast is updated with each new orbit determination from the navigation system. The simulation results presented in this section and the following section represent a control scenario using on-orbit CanX-4/-5 data as representative initial conditions from the navigation system. Table 2 summarizes the ROE states for the reconfiguration scenario.

Table 2: Initial and Desired ROE States with Error Between Achieved and Desired End State

ROE	Initial State, $\delta\boldsymbol{\alpha}_0$ [km]	Desired State, $\delta\boldsymbol{\alpha}_f$ [km]	Achieved Error, $\delta\boldsymbol{\alpha}_{err}$ [m]
δa	-0.719	0	1.08
$\delta\lambda$	1754	-150	171.60
δe_x	1.28	0	1.36
δe_y	1.16	-0.05	-3.79
δi_x	-0.28	0	1.11
δi_y	-0.02	-25	0.28

The reconfiguration scenario described in Table 2 is specified to complete in a 30 day period. The resulting guidance plan is shown by the ROE trajectories in Figure 6. This guidance plan represents the fuel-optimal reconfiguration based on the relative dynamics motion model discussed previously. For this particular scenario, an open-loop control period of two days is used, resulting in 15 intermediate configurations that are used as waypoints along the trajectory.

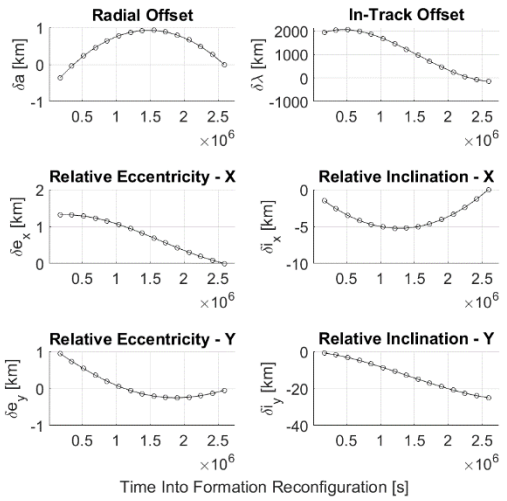

Figure 6: Formation Initialization Guidance Plan for the Complete ROE State

As one can see from Figure 7, the control solution computed from the guidance plan results in an ROE trajectory that very closely follows the fuel-optimal trajectory. The trajectory shown here is the result of the optimized control sequence being implemented in the high fidelity simulation model of STK, representative of on-orbit results. The simulated fuel expenditure was 16% greater than the calculated analytical minimum for this reconfiguration scenario. The difference between the achieved end state and the desired ROE is summarized in Table 2.

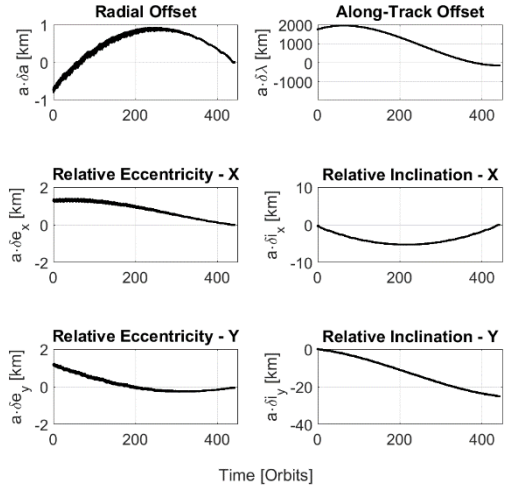

Figure 7: Simulated Reconfiguration Trajectory

A comparison between the performance of DRASTK and the updated GNC method, in terms of fuel-expenditure, is summarized in Table 3. For comparison, on-orbit results are used from the CanX-4/-5 formation initialization [1]. The updated GNC method was simulated using the same initial conditions, as computed using the navigation algorithm presented in this paper. A reconfiguration to the same desired end state of 3 km purely along-track separation was performed, and the initialization time was fixed to the identical period as the on-orbit initialization [1]. As previously noted, this reconfiguration period can be specified with the new GNC method – one of the added capabilities.

Table 3: Comparison of Updated Control Method to DRASTK for the CanX-4/-5 Initialization

	DRASTK	Updated GNC Method
Total Fuel Cost	2.03 m/s	1.71 m/s
Number of Maneuvers	102	565

It can be seen from Table 3 that the updated GNC method was more fuel-optimal than DRASTK. It is important to note that the simulation was restricted to a minimum spacing of 80 minutes between thrusts and that more than 5.5 times the number of maneuvers were performed compared to DRASTK. This is due to the numerical control method used and because the entire ROE state is being incrementally adjusted concurrently, instead of sequentially.

Station-keeping Simulation Results

Similar to reconfiguration, STK is employed within the station-keeping algorithm to provide a high fidelity simulation model of the formation. In addition to the benefits previously mentioned for reconfiguration, this allows for a more accurate prediction of fuel expenditure forecasted over a number of future station-keeping control periods.

The formation station-keeping scenario presented here is for maintaining the desired state configuration described in Table 2. The control period was a week long, with all control maneuvers restricted to the first few orbits of the period. The control bounds were set so maneuvers were targeted such that along-track drift did not exceed ± 0.5 km from -150 km desired $\delta\lambda$. Figure 8 displays the resulting ROE trajectory, forecasted to 12 station-

keeping periods from the end of the reconfiguration scenario.

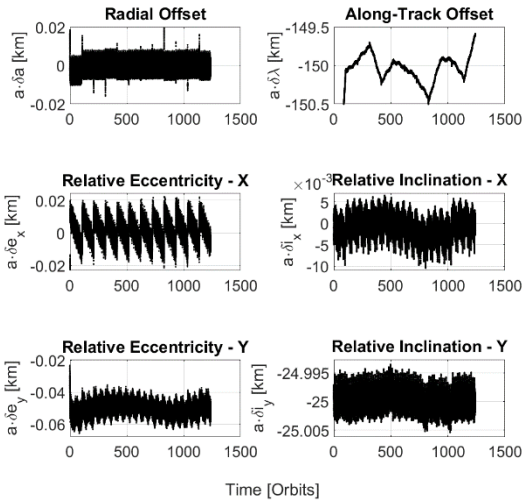

Figure 8: Simulated Station-Keeping Trajectory

The noisy appearance of the trajectories in Figure 8 is due to the use of Brouwer-Lyddane short mean elements to calculate the ROE state – these elements do not average-out longer periodic effects in the high-fidelity simulation environment. It can be seen from Figure 8 that along-track offset is maintained within the ± 0.5 km control bounds and drift in the x component of the relative eccentricity vector is centered about zero. The remaining ROE are maintained at their respective desired states specified in Table 2. Note that irregularity in along-track offset drift between consecutive station-keeping periods is attributed to minimum thrust constraints. If a required control thrust is below the minimum capability of the propulsion system, the maneuver can under- or overshoot the target – this is an imposed hardware limitation opposed to an algorithmic one. Lastly, the first station-keeping period has some ROE outside their control bounds due to a period of drift between the end of reconfiguration and beginning of station-keeping operations

As discussed previously, passive safety is ensured during a station-keeping control period through the relative separation of the $\delta \boldsymbol{e}$ and $\delta \boldsymbol{i}$ vectors. The more (anti-)parallel these vectors are, the more out of phase their respective harmonic oscillations are in the RN plane. Figure 9 demonstrates this passive safety during a single station-keeping control period by ensuring the relative phase of these oscillations remains closer to parallel than perpendicular, which would represent the satellites crossing the along-track axis with zero separation in the RN plane. Regardless of along-track separation, these two satellite trajectories will not intersect.

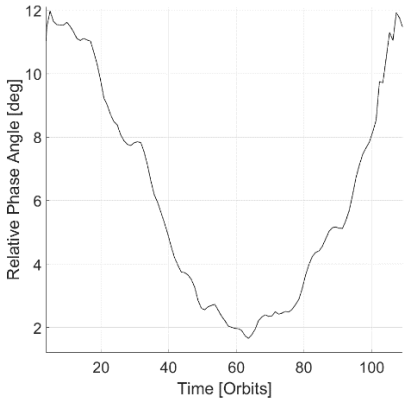

Figure 9: Passively Safe Separation of Relative Eccentricity and Inclination Vectors

Data in Figure 9 has been numerically averaged, over a sliding window of four orbits, to remove some longer period oscillations. This was done to make drift in relative phase angle over a station-keeping period clear.

FUTURE WORK

The next steps for the updated GNC system involve refinement of the operational process, estimation model and astrodynamics fidelity, and computational efficiency. Early mission operations will consist of updating GNC solutions with an operator in the loop to gain confidence in the system, and validate the relative dynamics model with on-orbit results. The next step is to further automate the GNC pipeline such that control solutions are updated on a continuing basis with new navigation information.

Refinement in the GNC system fidelity includes implementing finer processing of GPS data before it is input into the OD tool for better detection of outliers, and improving the fidelity of the relative dynamics motion model by including additional perturbations.

In its current state, the guidance system forecasts trajectories so that proximity risks can be determined by the operator. Passive safety is currently enforced by the algorithm at the end of reconfiguration and during station-keeping. However, an automated formation awareness procedure is in development that notifies the operator of an along-track proximity risk and automatically computes an alternative reconfiguration plan that mitigates that risk.

CONCLUSIONS

This paper has presented an updated ground-based GNC system that extends the capabilities of DRASTK to

distributed space systems for industrial applications. This includes: generalized reconfiguration for arbitrary formation geometries; station-keeping of along-track, cross-track, and radial formation baselines; and, consideration of operational time constraints.

CanX-4/-5 on-orbit data was used to evaluate the accuracy of the presented OD technique. This technique offers a streamlined navigation solution that provides adequate precision for distributed space systems that require control bounds on the order of a kilometer along-track and meters cross-track.

The updated GNC system provides fuel optimal maneuver solutions for fixed-time reconfiguration. A numerical optimization technique is implemented to plan guidance trajectories that reconfigure the complete ROE state concurrently over a specified time, while minimizing fuel expenditure. Additionally, station-keeping emphasizes payload operations by limiting formation control to a few orbits in the control period and leveraging drift in the ROE state to maintain baselines. Precision control capabilities are enabled by the relative motion model implemented with an STM that captures the Keplerian dynamics and J_2 perturbation effects. Additional perturbations can be included in the model through the GVE and augmented state parameters.

Building on the success of CanX-4/-5, this GNC system enables a wide range of distributed space systems, facilitating the next generation of small satellite missions.

ACKNOWLEDGEMENTS

The authors would like to acknowledge the contributions to this work and to CanX-4/-5 from many SFL staff and student; particularly, Dr. Robert E. Zee, Karan Sarda, Niels Roth, and Josh Newman. Niels Roth is further acknowledged for his insight and mentorship and Josh Newman for his work on DRASTK. Partners of the Hawkeye 360 Pathfinder mission are also gratefully acknowledged: HawkEye 360, Deep Space Industries, and GomSpace.

REFERENCES

[1] J. Newman, "Drift Recovery and Station Keeping Results for the Historic CanX-4/-5 Formation Flying Mission," in *29th Annual AISS/USU Conference on Small Satellites*, Logan, UT, 2015.

[2] T. P. Yunck, Global Positioning System: Theory and Applications - Orbit Determination, Washington, DC: AIAA Publications, 1996.

[3] N. Roth, "Navigation and Control Design for the CanX-4/-5 Satellite Formation Flying Mission," University of Toronto Institute of Aerospace Studies, Toronto, 2010.

[4] J. R. Wright, "Sequential Orbit Determination with Auto-Correlated Gravity Model Errors," *Journal of Guidance and Control,* vol. 4, no. 3, 1981.

[5] O. Montenbruk, O. Helleputte, R. Kroes and E. Gill, "Reduced Dynamic Orbit Determination Using GPS Code and Carrier Measurements," *Aerospace Science and Technology,* vol. 9, 2005.

[6] M. Mitchell, L. Breger and J. P. How, "Effects of Navigation Filter Properties on Formation Flying Control," in *AIAA Guidance, Navigation, and Control Conference and Exhibit*, Providence, Rhode Island, 2004.

[7] D. P. Scharf, F. Y. Hadaegh and S. R. Ploen, "A Survey of Spacecraft Formation Flying Guidance and Control (Part I): Guidance," in *American Control Conference*, 2003.

[8] J. Sullivan, S. Grimberg and S. D'Amico, "Comprehensive Survey and Assessment of Spacecraft Relative Motion Dynamics Models," *Journal of Guidance, Control, and Dynamics,* vol. 40, no. 8, pp. 1837-1859, 2017.

[9] A. W. Koenig, T. Guffanti and S. D'Amico, "New State Transition Matrices for Spacecraft Relative Motion in Perturbed Orbits," *Journal of Guidance, Control, and Dynamics,* vol. 40, no. 7, pp. 1749-1768, 2017.

[10] M. Chernick and S. D'Amico, "New Colosed-Form Solutions for Optimal Impulsive Control of Spacecraft Relative Motion," *Journal of Guidance, Control, and Dynamics,* vol. 41, no. 2, pp. 301-319, 2018.

[11] S. D'Amico and O. Montenbruck, "Proximity Operations of Formation-Flying Spacecraft Using an Eccentricity/Inclination Vector Separation," *Journal of Guidance, Control, and Dynamics*, vol. 29, no. 3, pp. 554-563, 2006.

[12] G. Gaias and S. D'Amico, "Generalised Multi-Impulsive Manoeuvres for Optimum Spacecraft Rendezvous in Near-Circular Orbit," *International Journal of Space Science and Engineering,* vol. 3, no. 1, pp. 68-88, 2015.

[13] C. W. T. Roscoe, J. J. Westphal, J. D. Griesbach and H. Schaub, "Formation Establishment and Reconfiguration Using Differential Elements in J2-Perturbed Orbits," *Journal of Guidance, Control, and Dynamics,* vol. 38, no. 9, pp. 1725-1740, 2015.